

MARIUSZ BARAŃSKI*

ELECTROTHERMAL ANALYSIS OF START-UP PROCESS IN THE SQUIRREL CAGE INDUCTION MOTOR USING FEM

POŁOWO-OBWODOWA ANALIZA ZJAWISK
ELEKTROMAGNETYCZNYCH I CIEPLNYCH PODCZAS
ROZRUCHU SILNIKA INDUKCYJNEGO MAŁEJ MOCY

A b s t r a c t

The paper presents a special algorithm and software for the analysis of coupled electromagnetic-thermal phenomena in a squirrel cage induction motor. In the proposed model the nonlinearity of the magnetic circuit, the movement of the rotor, the skewed slots and the influence of temperature on electrical and thermal properties of the materials have been taken into account. In order to verify the developed algorithm and software, the startup process of the motor has been examined, among others. The results of computations have been compared to the measurements.

Keywords: *electromagnetic and thermal field, squirrel cage motor, FE method*

S t r e s z c z e n i e

W artykule przedstawiono opracowany przez autora algorytm i oprogramowanie do analizy sprzążonych zjawisk elektromagnetycznych i cieplnych w silniku indukcyjnym klatkowym, Sg 100L-4B o mocy 3 kW. W opracowanym modelu zjawisk uwzględniono nieliniowość obwodu magnetycznego, ruch wirnika, skoszenie żłobków oraz wpływ temperatury na właściwości elektryczne i termiczne materiałów. W celu weryfikacji opracowanego algorytmu i oprogramowania przeprowadzono badania laboratoryjne. Przeprowadzono rozruch silnika indukcyjnego obciążonego momentem wynoszącym 12 Nm.

Słowa kluczowe: *zjawiska elektromagnetyczne i cieplne, silnik indukcyjny klatkowy, metoda elementów skończonych*

* Ph.D. Mariusz Barański, Electrical Machines and Mechatronics, Poznań University of Technology.

1. Introduction

Squirrel cage induction motors (IM) are still commonly used as industrial drives. The main benefits of IM are: simple design, construction, reliability of operation, low initial cost, easy operation and maintenance as well as relatively high efficiency. Because IM have a very important position in industry, therefore electromagnetic and thermal phenomena are required in the analysing and designing process of new IM.

Usually in the analysis of the transient operation of the squirrel cage motor the influence of the temperature on these processes is not taken into account. Nevertheless, in many cases this effect cannot be omitted, for example during the motor startup with a high inertia load or during operation with a partially damaged squirrel cage winding. Therefore, in order to increase the accuracy of the analysis of steady states and transients of the induction motors, the stator winding resistance, the squirrel winding conductivity as well as the thermal and magnetic properties of the materials should be considered as dependent on temperature [1–3, 9]. Commercial software programs (e.g. COMSOL Multiphysics, Ansys CFD) to simulate the dynamic operating conditions of electrical machines based on the two-dimensional or/and three-dimensional model of electromagnetic phenomena are more and more often used by scientific and research centers. The FEM analysis for a complex 3D problem is very time consuming and needs high-performance computing technology. However, a 3D model is necessary for a totally enclosed fan-cooled induction machine analysis. COMSOL Multiphysics and Ansys CFD enable to determine heat transfer coefficients.

In this paper, the author presents an elaborated algorithm and personally developed software for the analysis of the transients of an induction motor, taking into account the effect of temperature on the electrical, magnetic and thermal properties of materials in 2D.

2. Finite Element Formulation

The mathematical model of electromagnetic–thermal phenomena in a squirrel-cage motor includes equations of the electromagnetic field, the equation describing the distribution of the temperature field, the equations describing the dependence of resistivity and the thermal conductivity of materials on temperature. The model also includes the mechanical equilibrium equation of the studied electromechanical system. The problem was considered as two-dimensional and so-called field-circuit methods were used in the analysis of the squirrel-cage motor operation [2, 3, 10]. In order to describe the electromagnetic field, magnetic vector potential \mathbf{A} and electric potential V have been applied. The skew of slots was taken into account [1, 8]. The mathematical model after the space and time discretization can be written in the form of the following system of non-linear differential equations describing:

- the distribution of the magnetic field and currents in the windings:

$$\begin{bmatrix} \mathbf{S}_w + \mathbf{G}_w(1 - \mathbf{C}_{kw})p & -\mathbf{Z}_w \\ -\mathbf{Z}_w^T p & -(\mathbf{R} + p\mathbf{L}) \end{bmatrix} \begin{bmatrix} \mathbf{\Phi}_w \\ \mathbf{i} \end{bmatrix} = \begin{bmatrix} \mathbf{0} \\ -\mathbf{U} \end{bmatrix}, \quad (1)$$

- the distribution of temperatureL

$$(\mathbf{S}_\theta + \mathbf{K}_{\theta b} + \mathbf{G}_\theta p) \boldsymbol{\theta} = \mathbf{P} + \mathbf{K}_{\theta o}, \quad (2)$$

- angular velocity of the rotor:

$$J_b \frac{d^2 \alpha}{dt^2} + T_L(\alpha, t) + T_f(\varpi) = T_{el}(\alpha, \mathbf{A}) \quad (3)$$

where:

\mathbf{U}	– the vector of supply voltages,
\mathbf{i}	– the vector of loop currents,
Φ_w	– the vector of edge potentials,
$\boldsymbol{\theta}$	– the vector of nodal values of temperature,
\mathbf{S}_w	– the reluctance matrix,
\mathbf{G}_w	– the matrix of elementary conductance associated with the edges,
\mathbf{Z}_w	– the matrix that transforms the currents associated with the edges into loop currents i ,
\mathbf{C}_{kw}	– the coefficient of submatrices,
\mathbf{R}	– the diagonal matrix of winding resistances,
\mathbf{L}	– the matrix of end-turn inductances,
\mathbf{S}_θ	– the thermal conductivity matrix,
\mathbf{G}_θ	– the matrix of heat capacities,
θ	– the vector of nodal values of temperature,
\mathbf{P}	– the vector of nodal heat sources,
$\mathbf{K}_{\theta b}, \mathbf{K}_{\theta o}$	– the coefficients of matrices describing the heat transport to the surrounding of the motor, $p = d/dt$,
J_b	– the moment of inertia,
α	– the angle describing the rotor position,
ϖ	– the angular speed of the rotor,
$T_f(\varpi)$	– the breaking torque associated with movement of the rotor in viscous fluid and the friction in bearing $T_f(\alpha, t)$ is the load torque,
$T_{el}(\alpha, \mathbf{A})$	– the electromagnetic torque calculated on the basis of the magnetic field distribution [3].

Equations (1)–(3) of the presented model were solved simultaneously. To solve these equations the time-stepping method, the block relaxation procedure and the Newton-Raphson algorithm have been used [1, 3]. In order to shorten the calculation time, the different dynamics of electromagnetic and thermal phenomena can be taken into account in the algorithm. In the considered coupled problems, the winding resistance in (1) and the elements of matrix \mathbf{G}_w in (1) depend on temperature. Thus $\mathbf{R} = \mathbf{R}(\theta)$, $\mathbf{G}_w = \mathbf{G}_w(\theta)$.

Heat transfer occurs in three different modes, i.e. when temperature differences are present due to conduction, convection and radiation [3]. The major heat transfer at the boundaries of the induction motor occurs by conduction or convection. In the outer surface of the motor frame, heat is transferred mainly by convection, and the boundary condition is:

$$k \frac{\partial \theta}{\partial n} = -h(\theta - \theta_\infty), \quad (4)$$

where:

- k – the heat conductivity coefficient,
- h – the heat transfer coefficient,
- θ_∞ – the bulk temperature of the fluid.

The major difficulty in modelling is the determination of convection coefficient h . This scalar coefficient contains condensed information of the entire fluid flow model with mass and heat transport. In practical problems, this coefficient is estimated using dimensionless parameters describing the fluid conditions and containing geometrical information about the model. An accurate estimation of this coefficient is possible during a three-dimensional analysis or modelling, using Computational Fluid Dynamics (CFD) methods [4–6].

Here, in order to represent the transfer of heat in the winding end-regions, the equivalent heat transfer coefficient is applied. In the calculations of the equivalent heat transfer coefficient, the area of the end-winding region has been taken into account.

The author assumed that there were three types of heat sources:

- a) losses in windings ΔP_{Cu} ,
- b) eddy-current losses in cage bars ΔP_{Al} ,
- c) core loss ΔP_{Fe} .

The Joule losses in the stator windings are described by:

$$\Delta P_{Cu} = m(R_1)I^2 \quad (5)$$

where:

- m – the number of phases,
- R_1 – the stator winding resistance,
- I – the supply current.

The eddy current losses in the cage bars are written as follows:

$$\Delta P_{Al} = \frac{J^2}{\sigma_{Al}} \quad (6)$$

where the current density is calculated as $J = \sigma_{Al}(\text{grad } V - \partial \mathbf{A} / \partial t)$ and σ_{Al} is the aluminum conductivity that depends on temperature.

The core losses are:

$$\Delta P_{Fe} = k_B \Delta p_{B_0/f_0} \left(\frac{f}{f_0} \right)^{4/3} \left(\frac{B}{B_0} \right)^2 \rho_{Fe} k_{Fe} \quad (7)$$

where:

- k_B – the coefficient that takes into account the effect on the core losses other than the sample material, the magnetic field distribution in core,
- $\Delta p_{B_0/f_0}$ – the specific loss of used iron, calculated for B_0 and f_0 , f – the supply frequency,
- B – the amplitude of the fundamental harmonic of the time curve of the magnetic flux density in the core,
- ρ_{Fe} – the iron density,
- k_{Fe} – the core fill factor.

In the solution procedure, the equations of the field-circuit model and the FE equations of the thermal field have been considered as 2 blocks in an over relaxation block iterative procedure for solving a nonlinear algebraic equation. The Newton-Raphson method has been used to solve the equations of each block.

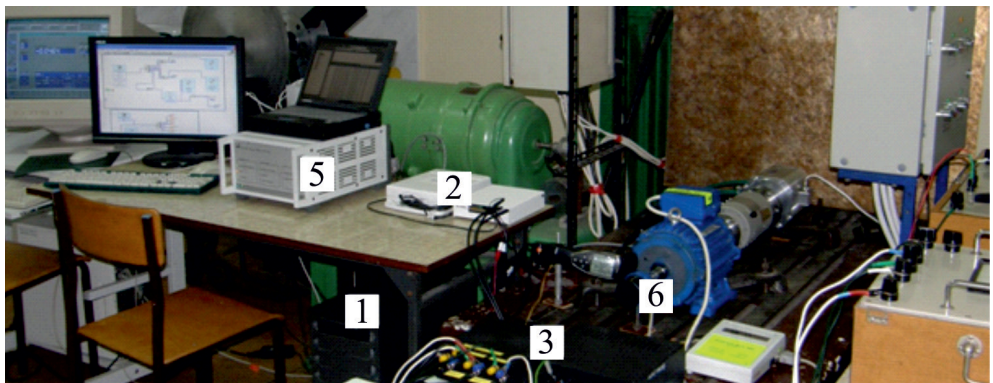
A detailed description of the mathematical model of electromagnetic-thermal phenomena in a squirrel-cage motor is presented in [1, 7, 8].

3. Results

The proposed algorithm of solving equations (1)–(3) has been applied in a computer program for the simulation of electromagnetic-thermal phenomena in a 3-phase, 4-pole, 3 kW squirrel-cage motor. The nominal data of the motor is: $U_N = 220/380$ V (D/Y), $f_N = 50$ Hz; $I_N = 12.0/6.9$ A, $n_N = 1415$ rpm. The stator winding data is as follows: 36 stator slots, 28 rotor slots, single layered. The start-up process of the motor has been analysed.

A test stand is shown in Fig. 1. The location of the PT100 sensors in a stator in order to measure the temperature distribution is shown in Fig. 2. The temperature measurement in the rotor winding was carried out by using a compact infrared thermometer – Fig. 3.

a)



b)

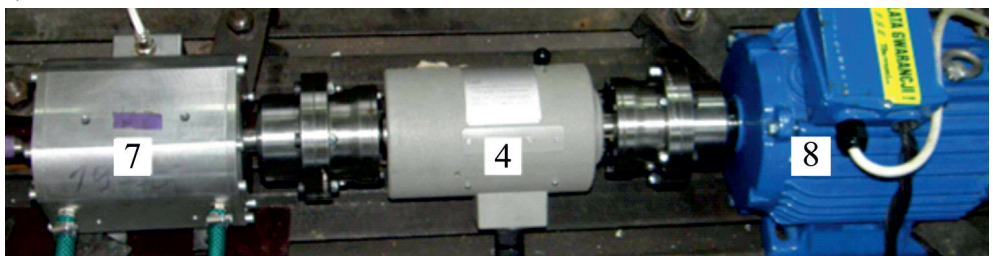


Fig. 1. Test stand: (1) PC computer with digital PCI cards; (2) and (3) LEM current and voltage, transducer; (4) and (5) torque transducer; (6) speed transducer; (7) magnetorheological, fluid break; (8) motor (a), power factor (b) and phase current (c) vs. load torque of the IM

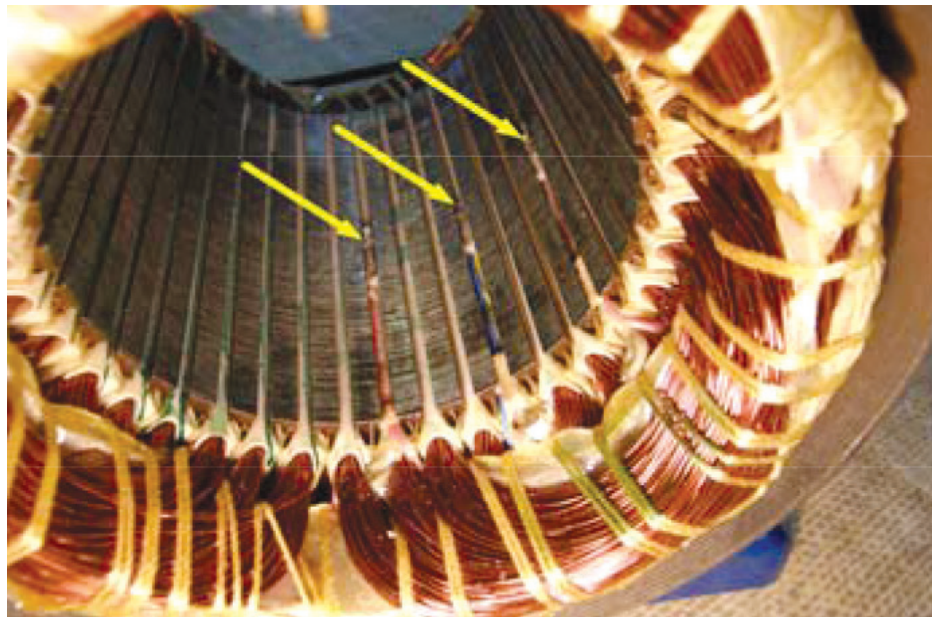


Fig. 2. Stator with PT100 sensors

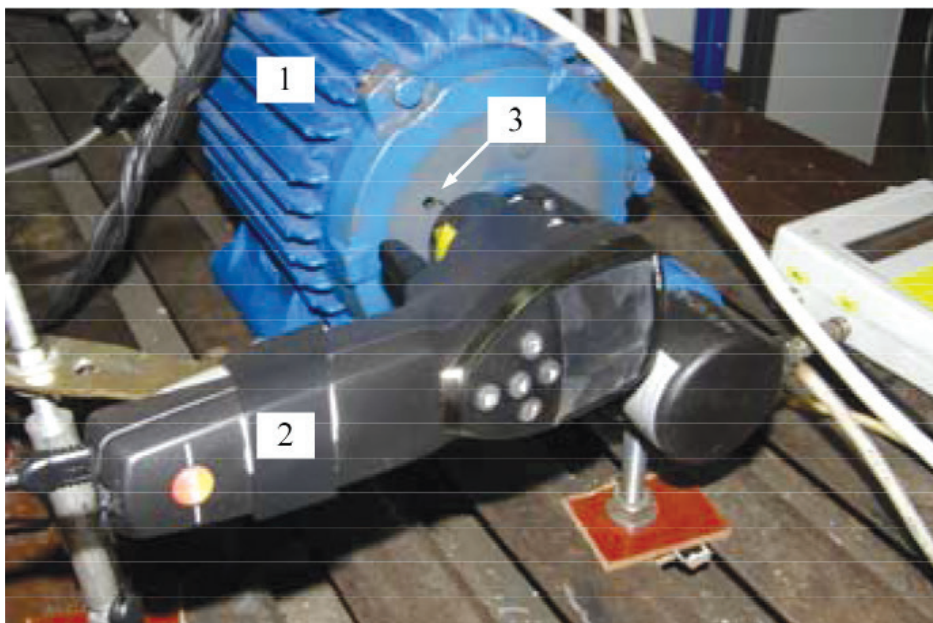


Fig. 3. Measuring the temperature of the ring, using a non-contact infrared thermometer:
1 – IM motor, 2 – measure device, 3 – hole in the bearing shield

Selected results of calculations are shown in Fig. 4–7. In the start-up test the amplitude of the supplied peak to peak voltage was decreased to 435 V and load torque T_L was equal to 12 Nm. The calculated torque (Fig. 5), current (Fig. 4) and speed of the motor waveforms (Fig. 6) have been compared with the results of measurements.

The magnetic field distribution and the temperature distribution in the motor have an impact on the distribution of the current density in the area of rotor cage bars. Fig. 7a shows the calculated distribution of the amplitudes of current density j along a rotor bar height for $t = 0.02$ s. Fig. 7b shows the temperature distribution in the rotor bar for $t = 0.02$ s. The calculations lead to the conclusion that the temperature rise in consecutive time steps, gradually increases the distribution of the current density [8]. This is caused by the non-uniform rise of temperature distribution in the rotor bar.

On the basis of the calculated magnetic field and temperature distribution, the schedules of the magnetic field and isotherms were plotted. Cross-sections of the motor in Fig. 8 show the electromagnetic (Fig. 8a) and temperature (Fig. 8b) distribution for $t = 0.02$ s, load torque T_L is equal to 12.

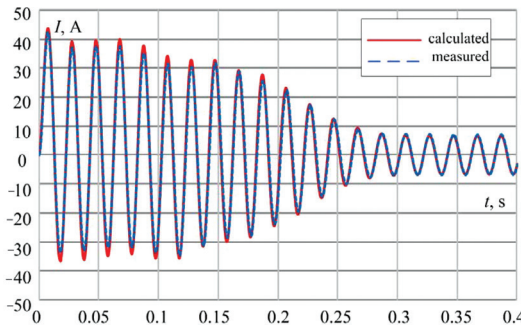


Fig. 4. Calculated and measured phase current time curves, $T_L = 12$ Nm

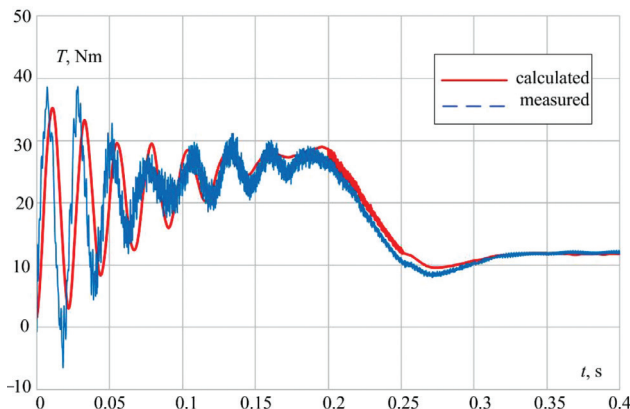
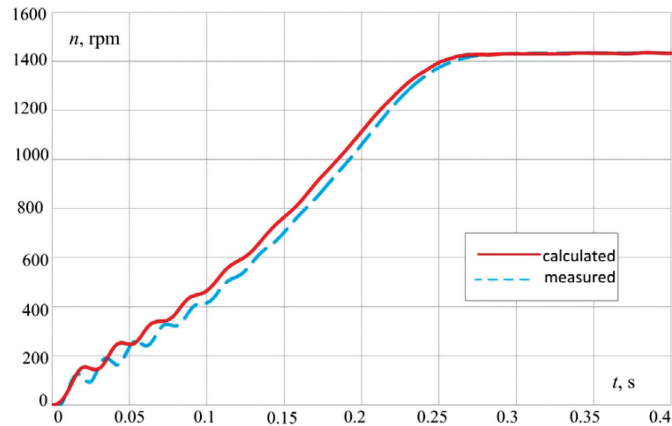
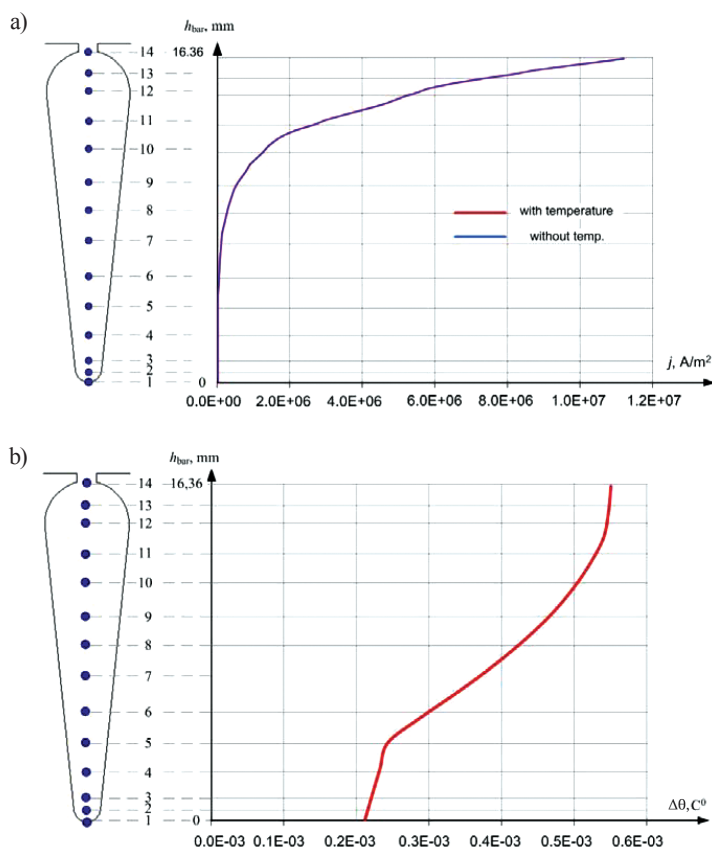


Fig. 5. Calculated and measured torque time curves, $T_L = 12$ Nm

Fig. 6. Calculated and measured speed time curves, $T_L = 12 \text{ Nm}$ Fig. 7. Distribution of current density j along height of the rotor bar (a) and temperature rise at selected points in rotor bar (b)

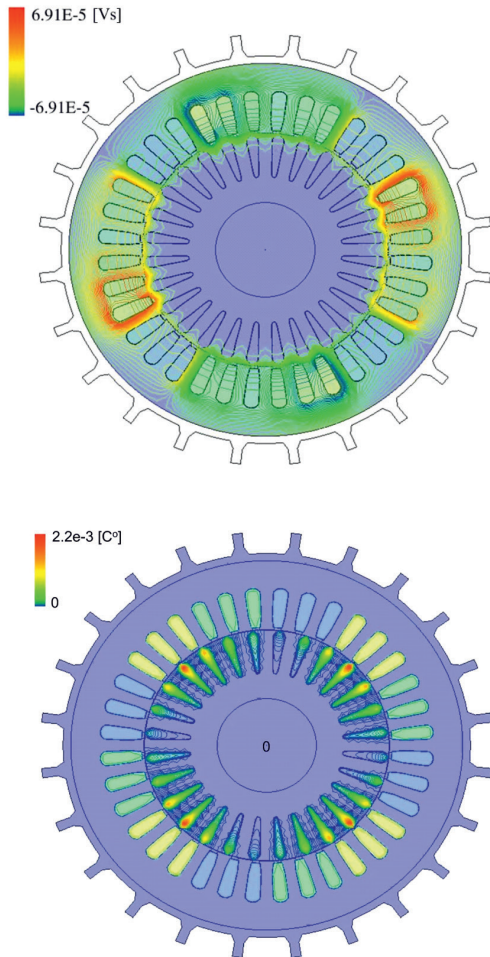


Fig. 8. Electromagnetic (Fig. 8a) and temperature (Fig. 8b) field distribution in cross-sections of the motor for $t = 0.02$ s

In Fig. 8a we can observe that due to the shielding effect of the rotor cage, temperature didn't have time to penetrate deep into the rotor. Whereas, Fig. 8b shows the rise of temperature distribution in the rotor bar during the start-up process.

4. Conclusions

This study highlights that the presented coupled model can be successfully applied to the analysis of transients of the squirrel cage induction motors. The obtained results and their comparison with the measurements show that the model is sufficiently accurate. The computerized stand for the measurement of transient electromagnetic and heat phenomena

in a motor of low power has been designed, built and tested. The elaborated computer software can be used to determine the parameters for designing functional and low power squirrel-cage induction motors as well as special squirrel-cage motors, e.g. motors working in cryogenic conditions.

References

- [1] Barański M., Szeląg W., *Finite element analysis of transient electromagnetic-thermal phenomena in a squirrel cage motor working at cryogenic temperature*. IET Science Measurement and Technology, Vol. 6, No 5, 2012, 1–7.
- [2] Hameyer K., Driesen J., De Gersem H., Belmans R., *The classification of coupled field problems*, IEEE Transaction on Magnetics, Vol. 35, No. 3, 1999, 1618–1621.
- [3] Driesen J., *Coupled electromagnetic-thermal problems in electrical energy transducers*, Katholieke Universiteit Leuven, 2000.
- [4] Kral Ch., Haumer A., Haigis M., Lang H., Kapeller H., *Comparison of a CFD Analysis and a Thermal Equivalent Circuit Model of a TEFC Induction Machine With Measurements*”, IEEE Transactions On Energy Conversion, Vol. 24, No. 4, 2009, 809–818.
- [5] Staton D., Hawkins D., Popescu M., *Motor-CAD Software for Thermal Analysis of Electrical Motors – Links to Electromagnetic and Drive Simulation Models*, CWIEME, Berlin, June 2010.
- [6] Pechanek R., Kindl V., Skala B., *Transient thermal analysis of small squirrel cage motor through coupled fea*, MM Science Journal, Vol. 03, 2015, 560–563.
- [7] Barański. M., *FE analysis of current displacement phenomena in a squirrel cage motor working at cryogenic temperature*, Archives of Electrical Engineering, Vol. 63, Issue 2, 2014, 139–147.
- [8] Barański M., Demenko A., Łyskawiński W., Szeląg W., *Finite element analysis of transient electromagnetic-thermal phenomena in a squirrel cage motor*, COMPEL – The International Journal for Computation and Mathematics in Electrical and Electronic Engineering, Vol. 30, No. 3, 2011, 832–840.
- [9] Arkkio A., *Analysis of induction motors based on the numerical solution of the magnetic field and circuit equations*, PhD thesis Acta Polytechnica Scandinava, Electr. Eng. Series No. 59, Laboratory of Electromechanics, Helsinki University of Technology, Helsinki 1987.
- [10] Martinez J., Belahcen A., Arkkio A., *A 2D FEM model for transient and fault analysis of induction machines*, Przeglad Elektrotechniczny, R. 88, Nr 7b, 2012, 157–160.